

Correlation of a Solution-State Conformational Change between Mercuric Chloride Complexes of Tris[(2-(6-methylpyridyl))methyl]amine with X-ray Crystallographic Structures

Deborah C. Bebout,* James F. Bush II, and Kathleen K. Crahan

Department of Chemistry, The College of William and Mary, Williamsburg, Virginia

Margaret E. Kastner and Damon A. Parrish

Department of Chemistry, Bucknell University, Lewisburg, Pennsylvania

Received March 16, 1998

Solution-state NMR and X-ray crystallography were used to investigate the complexation of HgCl_2 by the potentially tetradentate ligand tris[(6-methyl-2-pyridyl)methyl]amine (TLA) in acetonitrile. A change in the ligand conformation as a function of the metal-to-ligand ratio could be indirectly monitored through large changes in $^3J(^1\text{H}^{199}\text{Hg})$ to the methylene protons at -40°C . The solution-state NMR were correlated with two solid-state structures. The five-coordinate complex $[\text{Hg}(\text{TLA})\text{Cl}_2]$ (**1**) crystallizes in the triclinic space group $P\bar{1}$ with $a = 8.663(3)\text{ \AA}$, $b = 11.539(4)\text{ \AA}$, $c = 13.739(3)\text{ \AA}$, $\alpha = 80.81(2)^\circ$, $\beta = 75.84(2)^\circ$, $\gamma = 80.97(3)^\circ$, and $Z = 2$. The $\text{Hg}-\text{N}_{\text{amine}}$ distance of $2.505(7)\text{ \AA}$ for the tridentate ligand is the same as the average $\text{Hg}-\text{N}_{\text{lutidyl}}$ distance of $2.50(3)\text{ \AA}$ for the two bound lutidyl nitrogens. $[\text{Hg}(\text{TLA})\text{Cl}_2(\text{Hg}_2\text{Cl}_6)]$ (**2**) also crystallizes in $P\bar{1}$ with $a = 10.606(2)\text{ \AA}$, $b = 15.104(3)\text{ \AA}$, $c = 17.785(4)\text{ \AA}$, $\alpha = 67.46(3)^\circ$, $\beta = 83.52(3)^\circ$, $\gamma = 80.29(3)^\circ$, and $Z = 2$. The ligand is tetradentate in the two crystallographically unique cations which are arranged in a dimer-like orientation. The average $\text{Hg}-\text{Cl}$ distance is $2.37(1)\text{ \AA}$, and the average interionic $\text{Hg}-\text{Cl}$ distance is $3.51(1)\text{ \AA}$. The $\text{Hg}-\text{N}_{\text{lutidyl}}$ distances are of two types: two have an average distance of $2.36(3)\text{ \AA}$, nearly the same as the $\text{Hg}-\text{N}_{\text{amine}}$ distance of $2.35(2)\text{ \AA}$. The remaining four $\text{N}_{\text{lutidyl}}$ distances have an average distance of $2.56(5)\text{ \AA}$.

Introduction

An ideal structural metalloprobe would have ligand and coordination preferences comparable to the native metal while providing a sensitive spectroscopic handle. Nuclear magnetic resonance (NMR) is one of the most powerful spectroscopic methods because in addition to the chemical shift information which is indicative of the magnetic environment of an NMR active nucleus, it provides coupling constant information which identifies specific interacting nuclei and can often be related to geometric parameters. Numerous studies have shown that ^{113}Cd NMR is a powerful structural probe of oxygen-rich zinc and calcium protein metal binding sites.¹ Although NMR studies of ^{199}Hg -substituted proteins are currently much more limited,² $\text{Hg}(\text{II})$ maintains the d^{10} electron configuration of $\text{Cd}(\text{II})$ which minimizes intrinsic coordination geometry preferences while favoring coordination by softer ligands. The ^{199}Hg isotope has $I = 1/2$, comparable natural abundance and receptivity to ^{113}Cd , with larger chemical shift dispersion and shorter relaxation times. Heteronuclear coupling constants for ^{199}Hg in alkyl

mercurials³ have been determined to decrease in the order $^1J \gg ^3J > ^2J > ^4J$. However, the coupling constant data for small nitrogen coordination compounds of mercury is very limited.^{4–6}

We have been investigating the solution- and solid-state coordination chemistry of $\text{Hg}(\text{II})$ with a variety of dipodal and tripodal ligands containing nitrogen donors. These ligand systems simulate the geometric constraints imposed on the ligating residues of protein metal binding sites by tertiary protein structure. We recently reported studies with bis(2-methylpyridyl)amine (BMPA)⁵ and tris(2-methylpyridyl)amine (TPMA)⁶ in which $^3J(^1\text{H}^{199}\text{Hg})$ ranging from 20 to 80 Hz and $^4J(^1\text{H}^{199}\text{Hg})$ ranging from 20 to 24 Hz were observed. These values are comparable to those reported for $\text{Hg}(\text{II})$ -substituted proteins.² Trends in proton chemical shifts as a function of metal-to-ligand ratio reflected a series of equilibria between at least three complexes with these ligand systems. In an attempt to simplify

(1) Summers, M. F. *Coord. Chem. Rev.* **1988**, *86*, 43.

(2) (a) Utschig, L. M.; Bryson, J. W.; O'Halloran, T. W. *Science* **1995**, *268*, 380. (b) Utschig, L. M.; Wright, J. G.; Dieckmann, G.; Pecoraro, V.; O'Halloran, T. V. *Inorg. Chem.* **1995**, *34*, 2497. (c) Blake, R. P.; Lee, B.; Summers, M. F.; Park, J.-B.; Zhou, Z. H.; Adams, M. W. W. *New J. Chem.* **1994**, *18*, 387. (d) Marmorstein, R.; Carey, M.; Ptashne, M.; Harrison, S. C. *Nature* **1992**, *356*, 408. (e) Church, W. B.; Guss, J. M.; Freeman, H. C. *J. Biol. Chem.* **1986**, *261*, 234. (f) Cass, A. E. G.; Galdes, A.; Hill, H. A. O.; McClelland, C. E.; Storm, C. B. *FEBS Lett.* **1978**, *94*, 311.

(3) (a) Wrackmeyer, B.; Contreres, R. *Annu. Rep. NMR Spectrosc.* **1992**, *24*, 267. (b) Granger, P. In *Transition Metal Nuclear Magnetic Resonance*; Pregosin, P. S., Ed.; Elsevier: New York, 1991; p 306.

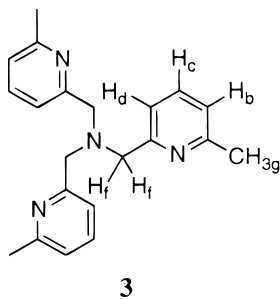
(4) (a) Schlager, O.; Wiegardt, K.; Grondey, H.; Rufinska, A.; Nuber, B. *Inorg. Chem.* **1995**, *34*, 6440. (b) Bashall, A.; McPartlin, M.; Murphy, B. P.; Powell, H. R.; Waikar, S. *J. Chem. Soc., Dalton Trans.* **1994**, 1383. (c) McWhinnie, W. R.; Monsef-Mirzai, Z.; Perry, M. C.; Shaikh, N.; Hamor, T. A. *Polyhedron* **1993**, *12*, 1193. (d) Nivorozhkin, A. L.; Sukhonenko, E. V.; Nivorozhkin, L. E.; Borisenko, N. I.; Minkin, V. I. *Polyhedron* **1989**, *8*, 569. (e) McCrindle, R.; Ferguson, G.; McAlees, A. J.; Parvez, M.; Ruhl, B. L.; Stephenson, D. K.; Wiecekowski, T. *J. Chem. Soc., Dalton Trans.* **1986**, 2351.

(5) Bebout, D. C.; DeLanoy, A. E.; Ehmman, D. E.; Kastner, M. E.; Parrish, D. A.; Butcher, R. J. *Inorg. Chem.* **1998**, *37*, 2952.

(6) Bebout, D. C.; Ehmman, D. E.; Trinidad, J. C.; Crahan, K. K.; Kastner, M. E.; Parrish, D. A. *Inorg. Chem.* **1997**, *36*, 4257.

these equilibria, we decided to investigate the effect of 6-methyl substitution on the solution behavior.

In this paper, our studies of the coordination chemistry of HgCl_2 with tris[2-(6-methylpyridyl)methyl]amine (TLA, **3**) are reported. The only previous study of TLA with Hg(II) involved



potentiometry and IR with less coordinating counterions.⁷ The structure of $[\text{Hg}(\text{TLA})\text{Cl}_2]$ and $[\text{Hg}(\text{TLA})\text{Cl}]_2(\text{Hg}_2\text{Cl}_6)$ are presented and compared to previously characterized mercuric complexes of 2-aminomethylpyridine-based ligands. Solution NMR studies in acetonitrile are also reported which support formation of related complexes in solution.

Experimental Section

Methods and Materials. All chemicals were obtained in reagent grade from Aldrich or Fisher except for 6-methyl-2-pyridine carboxaldehyde which was obtained from TCI America. FT-IR spectra were recorded in KBr pellets on a Perkin-Elmer 1600. Elemental analyses were carried out by Atlantic Microlab, Inc. (Norcross, GA).

Synthesis of tris[2-(6-methylpyridine)methyl]amine (TLA).⁸ TLA was prepared according to literature methods from 2-(6-methylpyridine)-methylamine⁹ and 2-chloromethyl-6-methylpyridine.¹⁰ The tan solid was recrystallized at least six times from hexanes to give colorless needles with mp 106–107 °C. ¹H NMR (CD_3CN): δ 7.58 (t, 3 H, J = 8 Hz, H_c), 7.40 (d, 3 H, J = 7.5 Hz, $H_{b,d}$), 7.04 (d, 3 H, J = 7.5 Hz, $H_{d,b}$), 3.74 (s, 6 H, H_f), 2.44 (s, 9H, H_g).

Synthesis of the Complex $[\text{Hg}(\text{TLA})\text{Cl}_2]$ (1). A solution of HgCl_2 (0.20 g, 0.75 mmol) in 2 mL of acetonitrile was added to a solution of TLA (0.5 g, 1.5 mmol) in acetonitrile (10 mL) with stirring. This solution was diluted with 8 mL of toluene and set aside for slow evaporation. Colorless plates formed in 2 days. Mp: 162–164 °C. ¹H NMR (2 mM, CD_3CN , 20 °C): δ 7.71 (t, 3 H, J = 7.5 Hz, H_c), 7.24 (d, 3 H, J = 7 Hz, $H_{b,d}$), 7.14 (d, 3 H, J = 7 Hz, $H_{d,b}$), 3.96 (s, 6 H, H_f), 2.71 (s, 9H, H_g). IR (KBr, cm^{-1}): 3062 w, pyridine C–H; 1601 s, 1591 s, 1574 s, py C=N; 1464 s, 1454 s, 1433 m, pyridine C=C; 2914 w; 1378 m; 1353 m; 1163 m; 1081 m; 1005 m; 992 m; 851 m; 800 m; 759 s; 649 m. Anal. Calcd for $\text{C}_{21}\text{H}_{24}\text{Cl}_2\text{HgN}_4$: C, 41.76; H, 4.00; N, 9.28. Found: C, 40.09; H, 3.83; N, 8.94.

Synthesis of the Complex $[\text{Hg}(\text{TLA})\text{Cl}]_2(\text{Hg}_2\text{Cl}_6)$ (2). A solution of TLA (99.5 mg, 299 μmol) in acetonitrile (2.5 mL) was added to an acetonitrile solution (2.5 mL) of HgCl_2 (244 mg, 897 μmol , excess necessary to avoid crystallization of **1**) with stirring. The solution was added dropwise to 250 mL of toluene and set aside for slow evaporation. Colorless needles of the complex formed upon standing for 4 days. Mp: 164.5–168 °C (dec). ¹H NMR (2 mM, CD_3CN , 20 °C): δ 7.78 (t, 3 H, J = 8 Hz, H_c), 7.31 (d, 3 H, J = 8 Hz, $H_{b,d}$), 7.23 (d, 3 H, J = 7.5 Hz, $H_{d,b}$), 4.09 (s, 6 H, $J(\text{HHg})$ = 78 Hz, H_f), 2.78 (s, 9H, H_g). IR (KBr, cm^{-1}): 3067 w, pyridine C–H; 1600 s, 1578 s, pyridine C=C; 1465 s, 1438 m, pyridine C=N; 2959 w; 2921 w; 2862 w; 1560 w; 1374 w; 1283 w; 1159 m; 1090 m; 1005; 786 s. Anal. Calcd for

Table 1. Selected Crystallographic Data

	$[\text{Hg}(\text{TLA})\text{Cl}_2]$ (1)	$[\text{Hg}(\text{TLA})\text{Cl}]_2(\text{Hg}_2\text{Cl}_6)$ (2)
empirical formula	$\text{C}_{21}\text{H}_{24}\text{N}_4\text{Cl}_2\text{Hg}$	$\text{C}_{42}\text{H}_{48}\text{N}_8\text{Cl}_8\text{Hg}_4$
fw	603.94	1750.84
space group	triclinic, $P\bar{1}$	triclinic, $P\bar{1}$
a , Å	8.663(3)	10.606(2)
b , Å	11.539(4)	15.104(3)
c , Å	13.739(3)	17.785(4)
α , deg	80.81(2)	67.46(3)
β , deg	75.84(2)	83.52(3)
γ , deg	80.97(3)	80.29(3)
V , Å ³	1304.6(7)	2590.1(9)
Z	2	2
d_{calc} , Mg/m^3	1.540	2.245
μ , cm^{-1}	61.16	122.269
radiation	Mo $K\alpha$	Mo $K\alpha$
(monochromatic)	(λ = 0.710 73 Å)	(λ = 0.710 73 Å)
T , °C	21	21
$R1^a$	0.0516	0.0840
$R2^b$	0.1639	0.2144

$$^a R1 = \sum ||F_o| - |F_c|| / \sum |F_o|. \quad ^b R2 = [\sum [w(F_o^2 - F_c^2)^2] / \sum [w(F_o^2)^2]]^{1/2}.$$

Table 2. Selected Bond Distances (Å) in $[\text{Hg}(\text{TLA})\text{Cl}_2]$ (1) and $[\text{Hg}(\text{TLA})\text{Cl}]_2(\text{Hg}_2\text{Cl}_6)$ (2)

	$[\text{Hg}(\text{TLA})\text{Cl}_2]$ (1)	$[\text{Hg}(\text{TLA})\text{Cl}]_2(\text{Hg}_2\text{Cl}_6)$ (2)	
Hg–N	2.505(7)	Hg1–N(A)	2.361(12)
Hg–N(1)	2.478(7)	Hg1–N1	2.341(14)
Hg–N(2)	2.513(6)	Hg1–N2	2.584(14)
Hg–Cl(1)	2.438(2)	Hg1–N3	2.497(14)
Hg–Cl(2)	2.408(3)	Hg1–Cl1	2.358(4)
		Hg2–N(B)	2.337(13)
		Hg2–N4	2.381(14)
		Hg2–N5	2.506(13)
		Hg2–N6	2.577(14)
		Hg2–Cl2	2.374(4)
N–C(F) _{av}	1.466(18)	N–C(F) _{av}	1.48(2)
N _{lu} –C(A) _{av}	1.362(8)	N _{lu} –C(A) _{av}	1.33(2)
N _{lu} –C(E) _{av}	1.331(6)	N _{lu} –C(E) _{av}	1.35(2)
C(E)–C(F) _{av}	1.499(18)	C(E)–C(F) _{av}	1.49(2)
		Hg _{anion} –Cl _{terminal,av}	2.368(11)
		Hg _{anion} –Cl _{bridging,av}	2.64(5)

$\text{C}_{42}\text{H}_{48}\text{Cl}_8\text{Hg}_4\text{N}_8$: C, 28.82; H, 2.76; N, 6.40. Found: C, 28.66; H, 2.82; N, 6.29.

X-ray Crystallography. Selected crystallographic data are given in Table 1, selected bond distances in Table 2, and selected bond angles in Table 3. Thermal ellipsoid plots are shown in Figures 1 and 2. Data were collected at 21 °C on a Siemens R3 four-circle diffractometer using graphite monochromated Mo $K\alpha$ X-radiation (λ = 0.710 73 Å). During data collection three standard reflections were measured after every 50 reflections. Both crystals turned black in the beam. The structures were solved by direct methods and Fourier difference maps using the SHELXTL-PLUS¹¹ package of software programs. Final refinements were done using SHELXL-93¹² minimizing $R2 = [\sum [w(F_o^2 - F_c^2)^2] / \sum [w(F_o^2)^2]]^{1/2}$, $R1 = \sum ||F_o| - |F_c|| / \sum |F_o|$, and $S = [\sum [w(F_o^2 - F_c^2)^2] / (n - p)]^{1/2}$. All non-hydrogen atoms were refined as anisotropic, and the hydrogen atomic positions were fixed relative to the bonded carbons and the isotropic thermal parameters were refined.

X-ray Diffraction of $[\text{Hg}(\text{TLA})\text{Cl}_2]$ (1). A semicircular plate measuring $0.40 \times 0.33 \times 0.20$ mm was glued on the end of glass fiber. Because a previous sample decomposed rapidly in the X-ray beam, faster ω scans were employed. The intensity of the standards dropped only 5% during this data collection, and all data were scaled on the basis of the standards. The final observed data-to-parameter ratio was 19:1.

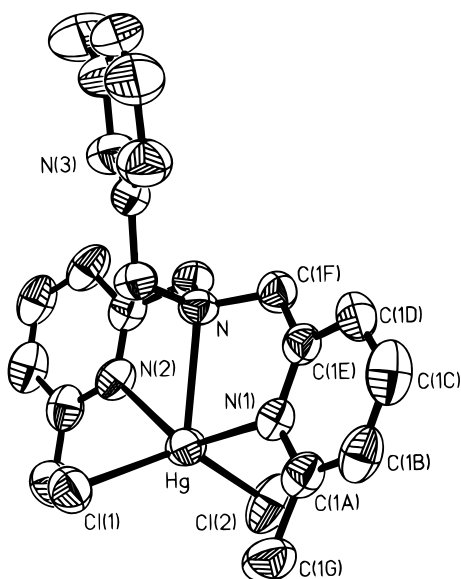
X-ray Diffraction of $[\text{Hg}(\text{TLA})\text{Cl}]_2(\text{Hg}_2\text{Cl}_6)$ (2). A colorless prism measuring $0.32 \times 0.12 \times 0.12$ mm was glued on the end of glass fiber.

- (7) Andereg, G.; Hubmann, E.; Podder, N. G.; Wenk, F. *Helv. Chim. Acta* **1977**, *60*, 123.
 (8) da Mota, M. M.; Rodgers, J.; Nelson, S. M. *J. Chem. Soc. A* **1969**, 2036.
 (9) Fuentes, O.; Paudler, W. W. *J. Org. Chem.* **1975**, *40*, 1210.
 (10) Jeromin, G. E.; Orth, W.; Rapp, B.; Weiss, W. *Chem. Ber.* **1987**, *120*, 9.

- (11) SHELXTL-Plus, Version 4.21/V; Siemens Analytical X-Ray Instr., Inc.: Madison, WI, 1990.
 (12) Sheldrick, G. M. *Crystallographic Computing*; Flack, H. D., Parkanyi, L., Simon, K., Eds.; Oxford University Press, 1993; Vol. 6, p 111.

Table 3. Selected Bond Angles (deg) in [Hg(TLA)Cl₂] (**1**) and [Hg(TLA)Cl]₂(Hg₂Cl₆) (**2**)

[Hg(TLA)Cl ₂] (1)		[Hg(TLA)Cl] ₂ (Hg ₂ Cl ₆) (2)	
N–Hg–N(1)	69.6(2)	N(A)–Hg1–N1	76.1(5)
N–Hg–N(2)	69.3(2)	N(A)–Hg1–N2	70.8(5)
N(1)–Hg–N(2)	138.9(2)	N(A)–Hg1–N3	70.7(5)
N–Hg–Cl(1)	106.9(2)	N(A)–Hg1–Cl1	158.4(4)
N–Hg–Cl(2)	117.6(2)	N1–Hg1–Cl1	125.2(3)
N(1)–Hg–Cl(1)	97.6(2)	N2–Hg1–Cl1	106.8(3)
N(2)–Hg–Cl(1)	95.7(2)	N3–Hg1–Cl1	109.7(3)
N(1)–Hg–Cl(2)	100.8(2)	N(B)–Hg2–N4	73.3(5)
N(2)–Hg–Cl(2)	96.5(2)	N(B)–Hg2–N5	70.8(4)
Cl(1)–Hg–Cl(2)	135.32(13)	N(B)–Hg2–N6	71.8(4)
		N(B)–Hg2–Cl2	166.9(4)
		N4–Hg2–Cl2	119.7(4)
		N5–Hg2–Cl2	104.7(3)
		N6–Hg2–Cl2	103.7(7)
Hg–N _{lu} –C(E) _{av(not 3)}	115.1(6)	Hg–N _{lu} –C(E) _{av}	111(2)
Hg–N–C(F) _{av}	106.2(5)	Hg–N _{am} –C(F) _{av}	108(2)
Hg–N _{lu} –C(A) _{av(not 3)}	125.2(1)	Hg–N _{lu} –C(A) _{av}	128(2)
C(A)–N _{lu} –C(E) _{av}	119.0(7)	C(A)–N _{lu} –C(E) _{av}	119.1(8)
		Cl _{term} –Hg _{an} –Cl _{term,av}	134(2)
		Cl _{term} –Hg _{an} –Cl _{bridg,av}	106(2)
		Hg3–Cl _{term} –Hg4 _{av}	88.6(5)

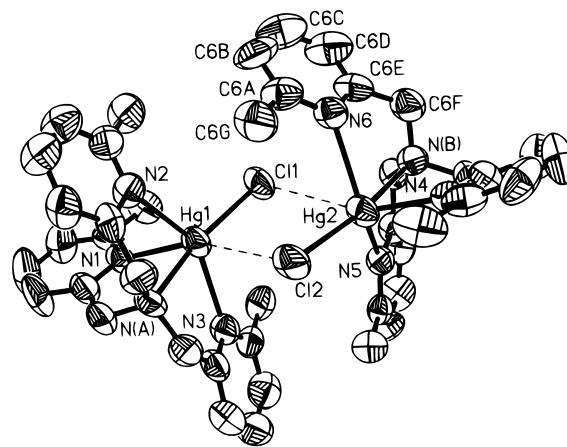
**Figure 1.** Thermal ellipsoid plot of [Hg(TLA)Cl₂] (**1**). Ellipsoids are at 50% probability. Hydrogens are omitted for clarity. Only one (6-methyl-2-pyridyl)methyl group is completely labeled.

The data were collected using the ω scan type due to rapid degradation in the X-ray beam. The intensity of the standards decreased about 28% during data collection, and all data were scaled on the basis of the standards. The final observed data-to-parameter ratio was 11:1.

NMR Measurements. All solutions for NMR titration analysis were prepared by adding stock solutions of mercuric chloride in acetonitrile-*d*₃ to solutions of TLA in acetonitrile-*d*₃ using calibrated autopipets. NMR spectra were recorded in 5-mm o.d. NMR tubes on a General Electric QE-300 operating in the pulse Fourier transform mode. The sample temperature was maintained by blowing chilled air over the NMR tube in the probe. The variable temperature unit was calibrated with methanol as previously described.¹³ Chemical shifts were measured relative to internal solvent but are reported relative to tetramethylsilane.

Results

Crystal Structure of [Hg(TLA)Cl₂] (1**).** The metal coordination sphere in **1** has distorted trigonal bipyramidal geometry.

**Figure 2.** Thermal ellipsoid plot of the two [Hg(TLA)Cl] cations in the asymmetric unit of **2**. Ellipsoids are at 50% probability. Hydrogens are omitted for clarity. Only one (6-methyl-2-pyridyl)methyl group is completely labeled.

The recently reported complex [CuCl₂(TLA)] has a similar, but less distorted, geometry.¹⁴ The only other structurally characterized example of tridentate metal-coordination by TLA is [Cd(TLA)(NO₃)₂].¹⁵ In **1** the two pyridyl nitrogens in the nominally axial positions form a N–Hg–N angle of 138.9°. The amine nitrogen and two chlorides form the equatorial plane. The Hg–N_{amine} distance of 2.505 Å is within the range of the Hg–N_{lutidyl} distances of 2.478(7) and 2.513(6) Å. A similar pattern is observed in the Cd(II) structure wherein the Cd–N_{amine} distance is 2.237 Å and the Cd–N_{lutidyl} distances are 2.369 and 2.390 Å. In [CuCl₂(TLA)] the Cu–N_{amine} distance is 2.145(6), 0.13 Å longer than Cu–N_{lutidyl} bond distances of 2.014(6) and 2.017(6) Å.

The Hg–N_{lutidyl} bond distances in **1** are slightly longer than the range previously reported for five-coordinate Hg(II) complexes involving ligation by pyridine derivatives.^{5,6} We recently reported approximate meridional coordination of the structurally related tridentate ligand bis(2-methylpyridyl)methyl]amine (BMPA) in the complex [Hg(BMPA)NCCCH₃](ClO₄)₂ (**3**).⁵ The somewhat longer (0.1–0.3 Å) Hg–N bond distances in **1** relative to **3** may be in part due to the increase in the coordination number from four to five.

Crystal Structure of [Hg(TLA)Cl]₂(Hg₂Cl₆) (2**).** The cations of **2** are crystallographically unique. Each is five-coordinate and highly distorted from either trigonal bipyramidal or square pyramidal geometry. The recently reported [CuCl(TLA)]⁺ complex has a very similar geometry and is the only other structurally characterized example of monomeric cations with tetradentate metal coordination by TLA.¹⁴ With the related pyridyl ligand system TMPA, nearly trigonal bipyramidal coordination has been observed in the complex [Hg(TMPA)Cl]₂(HgCl₄), with the Hg displaced about 0.76 Å below the plane of the N_{pyridyls} which form a nearly equilateral triangle.⁶ In both [CuCl(TLA)]⁺ and **2**, however, the N_{lutidyl} are not arranged as an equilateral triangle above the metal center. As can be seen in Figure 2, the lutidyl rings are clearly twisted such that the methyl groups are not symmetric about the Hg–Cl bond. This same asymmetry is seen in several dimeric structures of TLA with Fe(II).¹⁶ The Fe(II) structures are nearly octahedral with bridging oxide, hydroxide or fluoride ions completing the

(14) Nagao, H.; Komeda, N.; Mukaida, M.; Suzuki, M.; Tanaka, K. *Inorg. Chem.* **1996**, *35*, 6809.

(15) Xian-He, B.; Ahi-Hui, Z.; Zhi-Ang, Z.; Yun-Ti, C.; Huaxue, J. *J. Struct. Chem.* **1996**, *15*, 391.

(13) Raiford, D. S.; Fisk, C. L.; Becker, E. D. *Anal. Chem.* **1979**, *51*, 2050.

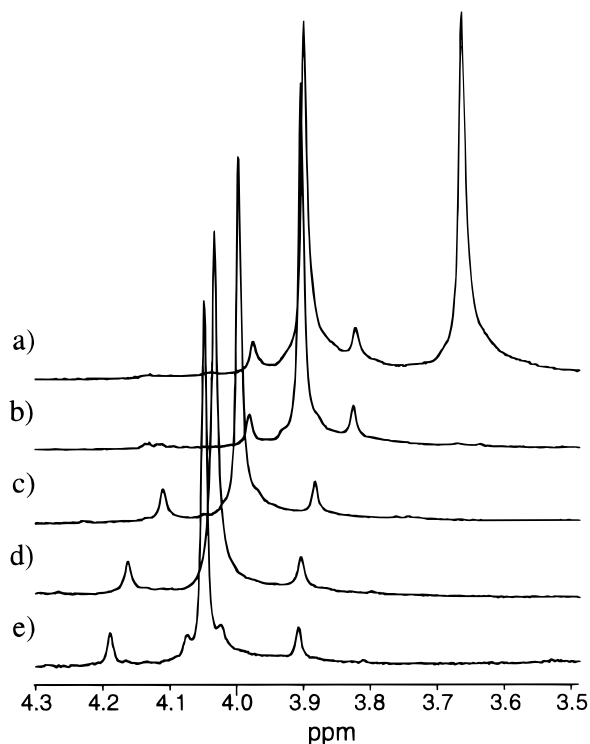


Figure 3. Methylene region (H_f) of the proton NMR spectra recorded at selected ratios of $HgCl_2$ -to-TLA in CD_3CN at -40 °C. The nominal concentration of $HgCl_2$ is fixed at 2 mM. $[HgCl_2]/[TLA] =$ (a) 0.5, (b) 0.75, (c) 1.0, (d) 1.25, (e) 1.5, (f) 3.0. Spectra are scaled to the height of the metal-bound ligand environment methylene peak.

coordination sphere. Figure 2 shows that in the solid state the two cations are arranged such that a dimeric structure is suggested. However, the $Hg-Cl_{bridge}$ distances of 3.51(1) Å are clearly nonbonding. In **2**, two of the lutidyl ligands are nearly coplanar and the crystallographically unique monomers pack such that these planes are nearly parallel and thus somewhat hindered. The $Hg-N_{lutidyl}$ distances in these ligands range from 2.34(1) to 2.58(1) Å. The less hindered $Hg-N_{lutidyl}$ distances and the $Hg-N_{amine}$ distances are nearly the same, ranging from 2.34(1) to 2.38(1) Å. Additionally, the $[CuCl(TLA)]^+$ cation is clearly monomeric and shows similar distortions with $Cu-N_{lutidyl}$ distances ranging from 2.03 to 2.16 Å.¹⁴

Investigation of TLA Coordination of $HgCl_2$ in the Solution State. Acetonitrile- d_3 solutions containing nominal molar ratios of TLA and $HgCl_2$ were examined by 1H NMR with total $[Hg(II)] = 2$ mM. Selected NMR spectra are shown in Figure 3. The chemical shifts of the individual 1H resonances and $^3J(^1H^{199}Hg)$ to the methylene hydrogens (H_f) as a function of $[Hg(II)]/[TLA]$ at -40 °C are shown in Figures 4 and 5, respectively. The NMR spectra for the $Hg(II)$ complexes at select metal-to-ligand ratios at -40 and 20 °C are shown in Figures S3 and S4 of the Supporting Information.

The first significant result of these studies is the slow exchange between bound and free ligand at low metal-to-ligand ratios and low temperatures. In contrast, under these conditions with the less sterically demanding ligand TMPA, exchange between bound and free ligand was rapid compared to the NMR time scale at temperatures as low as -40 °C.⁶ On the basis of the appearance of the discontinuities in the single set of observed chemical shifts and coupling constants for metal-bound TLA,

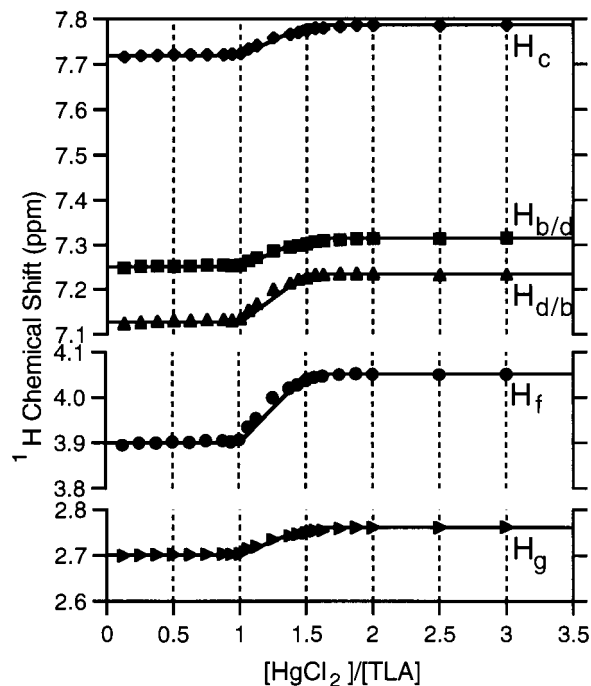


Figure 4. Chemical shifts of protons of TLA as a function of the nominal $HgCl_2$ -to-TLA ratio in CD_3CN at -40 °C. Chemical shifts of a second ligand environment consisting primarily of free ligand in the region below $[Hg]/[TLA] = 1.0$ are omitted for clarity. The nominal concentration of $HgCl_2$ is fixed at 2 mM. The lines represent the chemical shifts expected if interconversion of **1** and **2** was governed by equilibrium **2** with no intervening species and the equilibrium constant for both reactions **1** and **2** were highly favorable with $K_1 > K_2$.

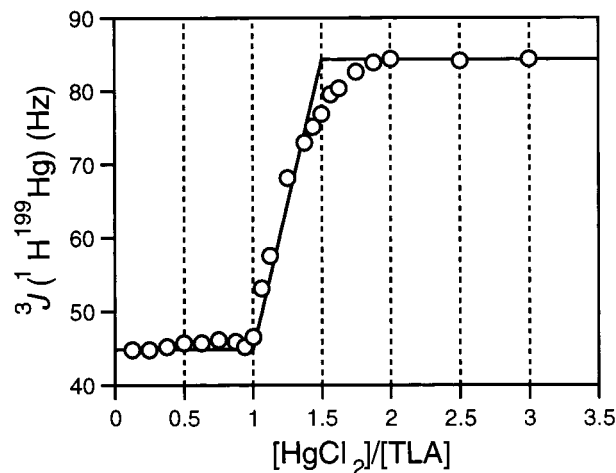
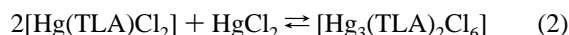
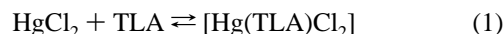


Figure 5. Magnitude of $^3J(^1H^{199}Hg)$ to the methylene protons (H_f) as a function of the nominal $HgCl_2$ -to-TLA ratio in CD_3CN at -40 °C. The nominal concentration of $HgCl_2$ was fixed at 2 mM. The line represents the coupling constant expected under the restrictions described for Figure 4.

equilibria described by the following stoichiometries are taking place:



As expected for a series of coupled equilibria of this type, the chemical shifts and heteronuclear coupling constants are nearly invariant outside of the transition region $1.0 < [Hg]/[TLA] < 1.5$. Within the transition region, the weighted average of the

(16) (a) Zang, Y.; Jang, H. G.; Chiou, Y.-M.; Hendrich, M. P.; Que, L., Jr. *Inorg. Chim. Acta* **1993**, *213*, 41. (b) Zang, Y.; Pan, G.; Que, L., Jr.; Fox, B. G.; Münch, E. *J. Am. Chem. Soc.* **1994**, *116*, 3653.

chemical shifts is expected to be described by eq 3

$$\delta_{\text{obs}} = P_{1:1}\delta_{1:1} + (1 - P_{1:1})\delta_{3:2} \quad (3)$$

where $\delta_{1:1}$ and $\delta_{3:2}$ are the chemical shifts and $P_{1:1}$ and $P_{3:2}$ [= 0.5(1 - $P_{1:1}$)] are the mole fractions of complexes with the respective metal-to-ligand stoichiometry. An equivalent expression would describe the trend in $^3J(^1\text{H}^{199}\text{Hg})$. The lines drawn in Figures 4 and 5 represent the expected chemical shift and coupling constant trends if both equilibria lie far to the right, reaction 1 is more favorable than reaction 2, and there are no intervening species. The data are consistent with the theoretical curves. The small chemical shift deviations in the transition region suggest that the actual sample concentrations are <5% higher than the nominal concentrations. Note that all the chemical shifts associated with Hg(II)-bound ligand were shifted downfield with respect to free ligand except one (H_b or H_d), a common result of the deshielding influence of σ donation to a metal cation.

The most striking feature of the solution NMR data is the preservation of the coupling between the methylene protons (H_f) and the metal center throughout the transformation between the species prevalent below 1:1 and above 3:2 metal-to-ligand ratios. The intensity of the coupling satellites relative to the main resonance were approximately $1/5$ the size of the main resonance at all metal-to-ligand ratios. Based on available precedent for coordination compounds of Hg(II)⁴ and alkylmercurials,³ the large magnitudes of the coupling constants suggest they arise through three-bond coupling rather than longer-range interactions. This implies that the Hg–N_{amine} bond is preserved throughout the transformation. To the best of our knowledge, this is the first time a solution-state conformational change of a ligand bound to Hg(II) has been monitored by following the NMR coupling between the metal and the ligand. Rapid exchange and the ability of Hg(II) to adopt many different coordination numbers with the same ligand type have precluded routine observation of this behavior.

The methylene protons of Hg(II)-complexed TLA were detected as an exchange averaged singlet with $^3J(^1\text{H}^{199}\text{Hg}) = 45$ and 81 Hz below 1:1 and above 3:2 metal-to-ligand solution ratios, respectively. In [Hg(BMPA)NCCH₃], the methylene protons were detected as a separate doublet of doublets with $^3J(^1\text{H}^{199}\text{Hg}) = 80$ and 41 Hz, reflecting slow exchange on the NMR time scale. A plausible interpretation of these observations, suggested by the structure of **1**, is that the Hg–N_{amine} bond remains intact on the NMR time scale while the Hg–N_{lutidyl} bonds are rapidly exchanged at low metal-to-ligand ratios. As a result of this exchange, all the methylene protons would be equivalent and show identical coupling while potential long-range coupling to the lutidyl protons would be lost. The magnitude of the $^3J(^1\text{H}^{199}\text{Hg})$ is identical to that observed in solution for a complex with stoichiometry [Hg(TMPA)Cl₂] whose structure has not been determined crystallographically. The later complex also exhibited $^3J(^1\text{H}^{199}\text{Hg}) = 24$ Hz coupling to the H_a protons, requiring that all nitrogen be bound to the Hg(II) on the NMR time scale. Unfortunately, TLA has a methyl group in this position and long-range coupling was not detected to any of the other lutidyl protons. As a result, additional information is required to assess ligation to the lutidyls in this complex. There are no known bidentate nitrogen ligands for which coupling has been reported to bound ^{199}Hg in solution.

The methylene coupling constant increases in the range 1.0 < [Hg]/[TLA] < 1.5 and remains 81 Hz at higher mole ratios. The average dihedral angles between the Hg(II) and the approximately anti and gauche TLA methylene protons are 162-

(15) and 80(16)^o in **2**. This is clearly much more restrictive than the range available when TLA is tridentate and there is rapid exchange between the bound and pendant lutidyl rings. Recently a Karplus-type relationship was suggested for the magnitudes of $^3J(^1\text{H}^{199}\text{Hg})$ which would predict weak coupling for torsion angles close to 90^o and the largest coupling for torsion angles that approach 0 or 180^o.^{2c} The methylene protons are equivalent, as observed in similar Hg(II) coordination studies of TMPA,⁷ consistent with conformational motions of the chelate rings interconverting the methylenes rapidly compared to the NMR time scale. The heteronuclear coupling constant to the methylene protons of TLA at high metal-to-ligand ratios is notably larger than for TMPA under similar conditions. As in the spectra collected at lower metal-to-ligand ratios, no coupling was detected between the other lutidyl protons and the metal center.

Discussion

A relatively limited number of metal complexes of TLA have been structurally characterized. The delicate interplay of factors leading to either tridentate or tetradentate TLA coordination had previously been demonstrated by structural characterization of the complex [Cu(TLA)Cl][Cu(TLA)Cl₂](ClO₄).¹⁴ In the diamagnetic HgCl₂ system, we were able to crystallize the tridentate and tetradentate ligand complexes separately and monitor their interconversion by NMR.

While correlations between solid-state structures and solution-state NMR properties must always be made cautiously,¹⁷ the simplicity of the NMR data is persuasive evidence for correlation with the solid-state structures of appropriate stoichiometry. All the chemical shifts move in the direction expected for reduction in the number of negatively charged chlorides bound to the ligand-associated Hg(II) at metal-to-ligand ratios exceeding 1:1. A survey of the relevant literature⁴ indicates that tridentate ligand coordination to a Hg(II) center appears to be minimally required for detection of coupling between ligand nuclei and ^{199}Hg in solution, even at low temperature. The conformational change associated with interconversion of tridentate and tetradentate TLA must occur with preservation of the Hg–N_{amine} coordination in order to maintain ^{199}Hg coupling to all the methylene protons.

The ability of Hg(II) to bind to varying numbers of donors in polydentate ligands frequently leads to complex solution equilibria. For example, explanation of our solution studies of TMPA with Hg(ClO₄)₂ over the metal-to-ligand ratio range investigated here required proposal of four Hg(II) complexes having different stoichiometry.⁶ Coupling between ^{199}Hg and the ligand nuclei could only be detected for the species with the highest and lowest metal-to-ligand ratio. Switching to chloride counterions in this system reduced the number of detectable species, but dramatically increased the rate of exchange with free ligand at low metal-to-ligand ratios, obscuring detectable coupling to all but an apparent 1:1 complex.

The HgCl₂/TLA system investigated here shows behavior intermediate between the Hg(ClO₄)₂/TMPA and HgCl₂/TMPA systems. Over the metal-to-ligand ratio examined, there was slow exchange between free ligand and a 1:1 metal-to-ligand species. The structure of **1** is fully consistent with the solution NMR data for the 1:1 complex as described in the Results. At solution metal-to-ligand ratios exceeding 3:2, a different ligand environment was prevalent. Cations with stoichiometry [Hg-(TLA)Cl] involving tetradentate TLA are suggested by the

(17) Davies, J. A.; Dutremez, S. *Coord. Chem. Rev.* **1992**, *114*, 201.

structure of **2**. Weak ion pairing in acetonitrile would be expected to produce insignificant differences in the proton NMRs of any [Hg(TLA)Cl] X salts. Our related study of [Hg-(TMPA)Cl]₂(HgCl₄)⁶ further supports the plausibility of this proposal, as does the known tendency of HgCl₂ to undergo complex speciation in solution.

Conclusions

We have identified a system in which a simple conformational change of a Hg(II)-bound ligand can be monitored by solution state NMR due to preservation of coupling between the metal center and protons of the ligand. This is particularly notable because literature precedent suggests extremely rapid exchange is a prevalent characteristic of Hg(II) complexes. This transformation was fully observable by NMR at low temperature where exchange with free ligand was slow on the NMR time scale. All NMR spectra were consistent with formation of complexes with average 3-fold symmetry and preservation of the Hg–N_{amine} bond on the NMR time scale. Two crystallographically characterized complexes provided plausible structures for the complexes prevalent at high and low [Hg]/[TLA].

Although only the methylene protons of TLA exhibited coupling to ¹⁹⁹Hg in this system, this supplementation of the chemical shift information permitted plausible structural assignment of solution-state complexes. The ³J(¹H¹⁹⁹Hg) assigned to solution-averaged versions of structures **1** and **2** differed by a factor of 2. This increase is consistent with a decrease in the range of H_f–C–N_{amine}–Hg dihedral angles available to the methylene protons in **2** compared to **1** and provides further support for development of a Karplus-type relationship for

³J(¹H¹⁹⁹Hg). Further documentation of this relationship by solid-state NMR of crystallographically characterized complexes of Hg(II) would permit ¹⁹⁹Hg scalar coupling information to be used in future distance geometry-based structure refinement strategies.

To the best of our knowledge, the preservation of coupling during a ligand conformational change has never been reported for small coordination compounds of Cd(II). Hg(II) may be unique in its ability to make strong bonds to nitrogen and yet accommodate facile ligand exchange. Further studies are needed to see if such characteristics are prerequisite for the preservation of coupling during ligand exchange. Should this be the case, the motivation to further exploit ¹⁹⁹Hg NMR as a metallobio-probe is increased by its potential usefulness in the investigation of equilibrium unfolding processes for Hg(II)-substituted proteins.

Acknowledgment. This research was supported by the Thomas F. and Kate Miller Jeffress Memorial Trust, by the donors of the Petroleum Research Fund, administered by the American Chemical Society, and by a Bristol-Myers Squibb Company Award of Research Corporation. The NSF-ILI program provided funding for the Bucknell University X-ray diffractometer.

Supporting Information Available: Figures S1–S4, showing thermal ellipsoid plots and additional NMR data, are available (4 pages). Two X-ray crystallographic files, in CIF format, are available on the Internet only. Ordering and access information is given on any current masthead page.

IC980296Y